Jestr

Journal of Engineering Science and Technology Review 17 (4) (2024) 40-49

Research Article

JOURNAL OF
Engineering Science and Technology Review

www.jestr.org

Experimental Study on High-Bonding Acrylic-polymer Waterproofing Materials

Dong Yan[1,2,3], Shuai Cheng[1,*], Xuedang Xiao[2], Lei Zhang[3] and Inchen Chen[4]

[1] *College of Architecture and Civil Engineering, Xinyang Normal University, Xinyang 464000, China*
[2] *Xinyang Lingshi Technology Co., Ltd, Xinyang 464000, China*
[3] *Yellow River Institute of Hydraulic Research, YRCC, Zhengzhou, 450003, China*
[4] *International College , Krirk University, Bangkok 10220, Thailand*

Received 16 April 2024; Accepted 16 July 2024

Abstract

Acrylic waterproofing materials are known for their excellent physical properties, waterproofing capabilities, and convenient construction, but their high cost and under-researched bonding strength pose challenges. To enhance adhesion and elucidate the imperviousness mechanism of engineering waterproofing materials while effectively controlling costs, this study proposed the compounding of acrylic ester polymer emulsion with low-cost styrene-acrylate copolymer emulsion for the preparation of waterproofing materials. By integrating theoretical analysis with experimental research, the physical and mechanical properties, as well as the imperviousness of the waterproofing materials, were investigated. The optimal mix-ratio design for the waterproofing materials was determined. Results demonstrate that, (1) The compounding of styrene–acrylic emulsion with pure-acrylic emulsion can achieve good performance while lowering costs. (2) The common silicate cement strength 42.5MPa (C42.5) had better comprehensive properties than the common silicate cements strength 32.5MPa (C32.5) and 52.5MPa (C52.5) and the rapid-hardening sulfate–aluminate cement. (3) In the imperviousness and bonding-strength tests of the coating, when the waterborne non-silicone defoamer was added at 0.3%, it was dense inside the coating with reduced microspaces, and the coating passed the imperviousness test after 30 min under a water pressure of 0.3 MPa. (4) The bonding strength with cement-based surfaces was 1.8 MPa. This study can serve as a good reference for research on high-bonding waterproofing coatings of acrylic acid for underground engineering applications and imperviousness-performance tests.

*Keywords:*Acrylic-polymer waterproofing materials, Two-component, High-bonding, Waterproof and impermeable, Underground engineering

1. Introduction

As the construction scale of above-ground buildings and structures approaches saturation, underground engineering has commenced to play a pivotal role in engineering, with research initiatives on underground engineering [1] sprouting nationwide. As the economy gallops forward, metropolitan areas are faced with a paucity of usable above-ground space. Thus, they have initiated explorations below ground. The swift evolution of urbanization has given rise to a proliferation of subways, underground parking lots, and underground commercial streets. These structures foster the expedited growth of cities and mitigate issues such as the scarcity of underground space. A key distinction between underground and above-ground engineering lies in the approach to leakage prevention. To address leakage issues, above-ground engineering projects incorporate a combination of waterproof and drainage measures, such as the installation of drainage ditches, drainage wells, and leakage trenches to prevent leakage. Conversely, underground engineering cannot be dealt with in the same manner due to its typical positioning at or below the underground water level [2]. The impact of underground water on the leakage of underground structures is significantly greater than that on above-ground engineering. Thus, leakage is consistently one of the primary issues leading to the deterioration of underground engineering structures.

With the introduction of requirements for high-quality development, the requirements for engineering quality is further elevating, and the issue of engineering leakage urgently requires resolution [3]. Currently, the primary measure for preventing leakage in underground engineering involves paving SBS waterproofing membranes during construction, which can provide a certain degree of protection for the water resistance and impermeability of basements. However, this measure is costly, not environmentally friendly, and requires the use of hot-melting methods for paving membranes, which pose a fire hazardand can injure workers during construction [4]. Upon the conclusion of simultaneous construction, the overlapping joints are prone to water leakage during rainy seasons and in winters, failing to effectively prevent the infiltration of water. Over time, SBS membranes can become detached due to poor adhesion. The detachment leads to peeling off, which can result in the deterioration of underground engineering and affecting the service life of underground engineering [5].

To address the issues of poor bonding strength and leakage at joints and seams of SBS membranes used for waterproofing in current underground engineering, the current study proposed a method for preparing a green, environmentally friendly, non-toxic, and harmless high-bonding acrylate polymer waterproofing coating. An experimental model for this high-bonding acrylate polymer waterproofing coating was also established to analyze and investigate the water resistance and impermeability and bonding-strength properties of this new type of high-

*E-mail address: chengshuaijs@163.com
ISSN: 1791-2377
doi:10.25103/jestr.174.06

bonding acrylate polymer waterproofing coating for underground engineering. Through the analysis and investigation of physical properties and characteristics, we aimed to accurately reveal the water resistance and impermeability effect of high-bonding acrylate polymer waterproofing coatings and address the issue of leakage in underground engineering due to insufficient adhesion. Our work can serve as a reference for the application of high-bonding acrylate polymer waterproofing coatings in the water resistance and impermeability fields for underground engineering and personalized use.

2. State of the art

Polymer-cement waterproofing coatings have been extensively studied. These materials are deeply trusted and recognized by construction personnel of underground engineering due to their advantages of being non-toxic, harmless, green, environment friendly, and cost effective, as well as their ease of application and excellent water resistance and impermeability properties [6]. Yan [7] examined on the problems encountered in the practical application of waterproofing coatings, considering the amount of emulsion used, construction conditions, and the coated working surface. However, they used functionally limited polymer-cement waterproofing coatings and focused solely on waterproofing performance. Wu [8] explored the impact of the dosage of waterborne micro-nano graphite slurry, i.e., the mass ratio of polymer waterproofing coating to cement, on the various physical and mechanical properties of the waterproofing coating. However, no systematic test of the bonding strength in actual engineering is conducted. Cheng [9] modified a waterproofing coating with an environment-friendly crosslinker derivative of methyl propiolate (HA). They discussed the impact of the ratio and amount of compounding emulsifying agents, the amount of initiator, and the amount of HA on the performance of the waterproofing coating. However, the technology is complex and bonding strength is not discussed. Czarnecki [10] focused on optimizing the elastic polymer-cement protection coating composition using material model. The material model consists of mathematical relations between composition and technical features demanded for protection.

Wang [11] decided to clarify the effect and influence mechanism of polymers on the waterproof performance of cement mortar and studied the effects of three polymers on capillary water absorption, impermeability, porosity and cracking of cement mortar. Kim [12] confirmed that the protection of crack-shielding property can enhance water tightness, offering a reference for improving the bonding strength of waterproofing coatings. Lee [13] enhanced the waterproof performance by incorporating sheet-adhesion techniques in composite-material construction and applying high-polymer waterproof materials on-site, providing a reference for addressing the issues of bubble formation and uneven thickness during the construction process. Meng [14] developed an environment-friendly, fluorine-free waterproof hybrid coating by using vinyltributoxysilane as a functional monomer and octyltriethoxysilane-modified SO_2 as inorganic filler. The fluorinated coatings are environmentally protective ones, offering a reference for outdoor applications. Liu [15] prepared SBS-modified emulsified asphalt and SBR-modified emulsified asphalt with different asphalt ratios. They explored the effects on the flow time, air content and mechanical properties of cement-emulsified asphalt mortar. Al-Zahrani [16] conducted an accelerated corrosion test on concrete specimens coated with polymer-based, cement-based polymer-modified and cement-based waterproofing coatings to determine the onset of corrosion, offering a reference for integrated design. Marques [17] experimentally studied the behavior of self-protective particles in asphalt films under environmental degrading agents, modified asphalt films with non-oriented polypropylene and styrene–butadiene–styrene. They assessed the adhesion of the self-protective particles, proposing suggestions for waterproofing-coating development. Yu [18] synthesized modified waterborne polyurethane by self-emulsification and studied the mechanism of contact-angle improvement, offering a reference for using waterborne polyurethane as a waterborne waterproofing coating. Jassal [19] studied the performance of environment-friendly waterborne polyurethane dispersions in waterproof breathable coatings by assessing the properties, number of coatings, and influence of additives, presenting a method for subsequent coatings to include polymer adhesives for durability enhancement.

The above studies have focused primarily on the modification and mechanism analysis of different types of waterproofing coatings in terms of imperviousness and durability, merely satisfying one aspect of the performance requirements. Less emphasis is given to the study and modification of the tensile strength, elongation at break, and bonding strength of waterproofing coatings. Particularly, research on the bonding strength of waterproofing coatings to concrete surface layers in underground engineering is lacking. Using a precast-mortar substrate method, the present work established a model for the bonding strength of waterproofing coatings. From the multi-performance direction of waterproofing coatings, we discussed the advantages of the developed high-bonding acrylic cement waterproofing coating and plaster in terms of impermeability, bonding strength with the substrate, tensile strength, elongation at break, and imperviousness. The coupling relationship between the acrylic-cement waterproofing coating and the bonding strength to the mortar substrate was inferred, providing a basis for the application and modification of acrylic-cement waterproofing coatings.

The remainder of this study is organized as follows. Section 3 describes the design of an orthogonal test plan with three factors and four levels to determine the physical and mechanical properties and bonding strength of the waterproofing coating. The initial ratio of the waterproofing coating was determined. Section 4 explores the impact of the selection of different grades of cement on the physical and mechanical properties of the waterproofing coating and the effect of the defoamer dosage on the water resistance and impermeability properties of the waterproofing coating. The grade of cement and defoamer dosage that yielded the optimal performance of the waterproofing coating was determined. The final section summarizes the entire paper and presents the conclusions of the experimental analysis.

3. Methodology

3.1 Test scheme

The orthogonal test plan determined the initial ratio by a three-factor four-level orthogonal test (Table 1 Orthogonal Test Plan Table), with the percentage of pure-acrylic emulsion in the liquid component, the percentage of styrene–acrylic emulsion in the liquid component, and the

percentage of cement in the powder component serving as the three factors of the orthogonal test, investigating the tensile strength, elongation at break, and bonding strength of each ratio. The percentages of dispersant, defoamer, and thickener in the liquid component were fixed at 0.2%, 0.3%, and 0.3%, respectively. The solid components included cement, 80–120 mesh quartz sand, 200 mesh quartz sand, 400 mesh heavy calcium carbonate, 800 mesh heavy calcium carbonate, and 1250 mesh talc powder. Each solid component accounted for 35%, 30%, 15%, 12%, 6%, and 2% of the solid component, respectively. In this phase, the mass ratio of the liquid component to the solid one (referred to as the liquid–powder ratio) was 1:1.5.

Table 1. Orthogonal Test Plan Table

Example	A: Styrene–Acrylic Emulsion (Parts)	B: Pure-acrylic emulsion (Parts)	C: Cement (Parts)
1	21	55	35
2	21	60	40
3	21	65	45
4	21	70	50
5	24	55	40
6	24	60	35
7	24	65	50
8	24	70	45
9	27	55	45
10	27	60	50
11	27	65	35
12	27	70	40
13	30	55	50
14	30	60	45
15	30	65	40
16	30	70	35

Inorganic Filler-Modification Test Plan: The performance-optimized group 11 from the orthogonal test was selected to investigate the impact of ordinary silicate cements C32.5, C42.5, C52.5, and the rapid-hardening sulfate–aluminate cement on the physical and mechanical properties and water resistance and impermeability properties, determining the optimal cement grade. When the mass ratio of cement was too high, the hydration reaction during film formation of coatings was severe, making film formation difficult and prone to uneven cracking. Thus, C42.5 ordinary silicate cement was selected, with the other components maintaining their original mass ratio.

3.2 Test Materials and Instruments

The liquid components included styrene–acrylic copolymer emulsion (referred to as styrene–acrylic emulsion), acrylic polymer emulsion (referred to as "pure-acrylic emulsion"), polymeric carboxylic acid ammonium salt dispersant, waterborne non-silicone defoamer, alkali-swelling thickener, carson fungicide, and deionized water. The solid components included 32.5MPa, 42.5MPa, and 52.5MPa common silicate cement (the following expressions were C32.5, C42.5 and C52.5), rapid-hardening sulfate–aluminate cement, 80-120 mesh quartz sand, 200 mesh quartz powder, 400 mesh, 800 mesh heavy calcium carbonate, and 1250 mesh talc powder.

The primary testers used were impermeability tester, imperviousness tester, tensile-testing machine, coating frame, sheet-punching machine, dumbbell-shaped cutter, thickness gauge, and mixer.

3.3 Test Method for Bonding Strength

The liquid components included styrene–acrylic copolymer emulsion (referred to as styrene–acrylic emulsion), acrylic polymer emulsion (referred to as “pure-acrylic emulsion”), polymeric carboxylic acid ammonium salt dispersant, waterborne non-silicone defoamer, alkali-swelling thickener, carson fungicide, and deionized water. The solid components included 32.5MPa, 42.5MPa, and 52.5MPa ordinary Portland cement grades (the following expressions were C32.5, C42.5 and C52.5), rapid-hardening sulfate–aluminate cement, 80–120 mesh quartz sand, 200 mesh quartz powder, 400 mesh, 800 mesh heavy calcium carbonate, and 1250 mesh talc powder.

The primary testers used were impermeability tester, imperviousness tester, tensile-testing machine, coating frame, sheet-punching machine, dumbbell-shaped cutter, thickness gauge and mixer.

$$T_L = \frac{P}{B \times D} \tag{1}$$

where T_L is the tensile strength in megapascals (MPa), P is the maximum tensile force in newtons (N), B is the width at the middle part of the specimen in millimeters (mm), and D is the specimen thickness in millimeters (mm).

The calculation formula for elongation at break is

$$E = \left(L_1 - L_0\right) \Big/ L_0 \times 100\% \tag{2}$$

where E is the elongation at break in percentage (%), L_0 is the initial distance between marking lines on the specimen (25mm), and L_1 is the distance between marking lines at the time of specimen fracture in millimeters (mm).

The test was conducted under standard conditions (23℃, relative humidity: 50%) with the specimen placed horizontally. The surface was coated with high-strength adhesive, and the bonding strength was measured using a clamp (Fig. 2) to ensure tight adhesion (Fig. 3). The bonding-strength test determined the maximum tensile force F. The bonding strength was calculated using the following formula:

$$\sigma = \frac{F}{1600} \tag{3}$$

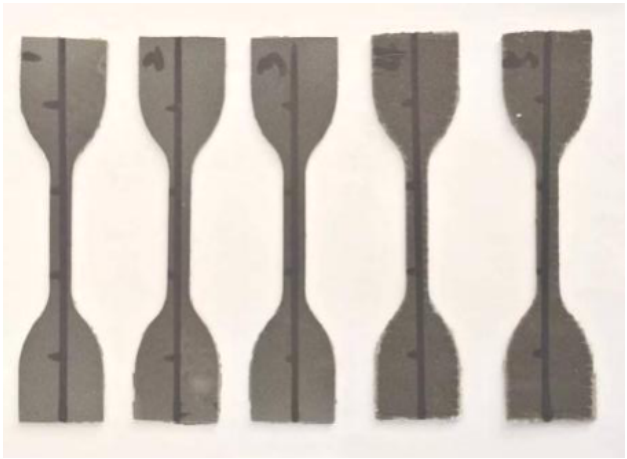

Fig 1. Dumbbell-Shaped Specimen

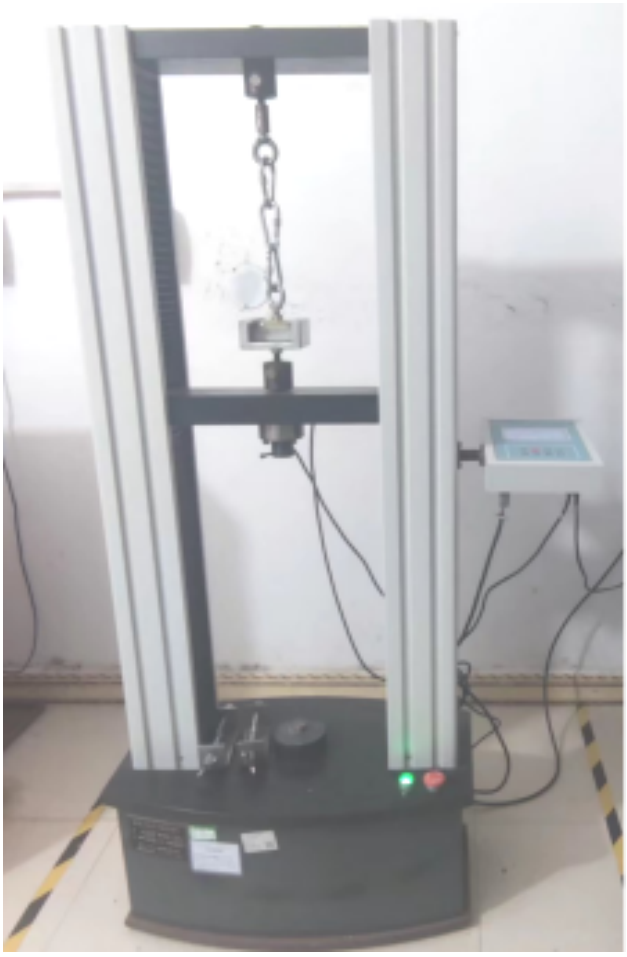

Fig. 2. Tensile and Adhesion Testing Machine

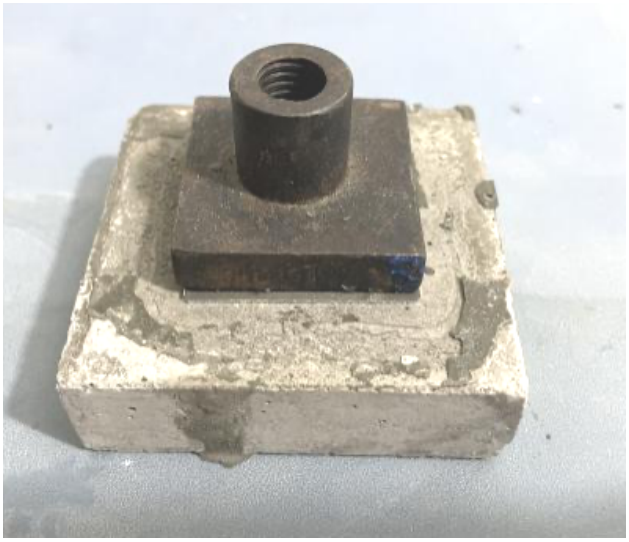

Fig. 3. Detailed View of Bonding Strength

3.4 Test Method for Imperviousness

The imperviousness test was referenced from the Chinese Test Methods for Building Waterproofing Coatings (GB/T 16777-2008). Three specimens with dimensions of 150mm × 150mm × 1.5mm were cut from the film cured to the specified age as per 3.3 and reserved for use. The air inside the imperviousness tester (Fig. 4) was exhausted, and the specimens were placed on the pervious disc of the testing machine (Fig. 5). A metal mesh and a seven-hole disc were placed on the specimen cover, and the specimen was clamped and slowly pressurized by the machine. The water pressure was increased to 0.3MPa and maintained for 30min. If no water seepage occurred on the non-water-facing side, the specimen was deemed to be qualified.

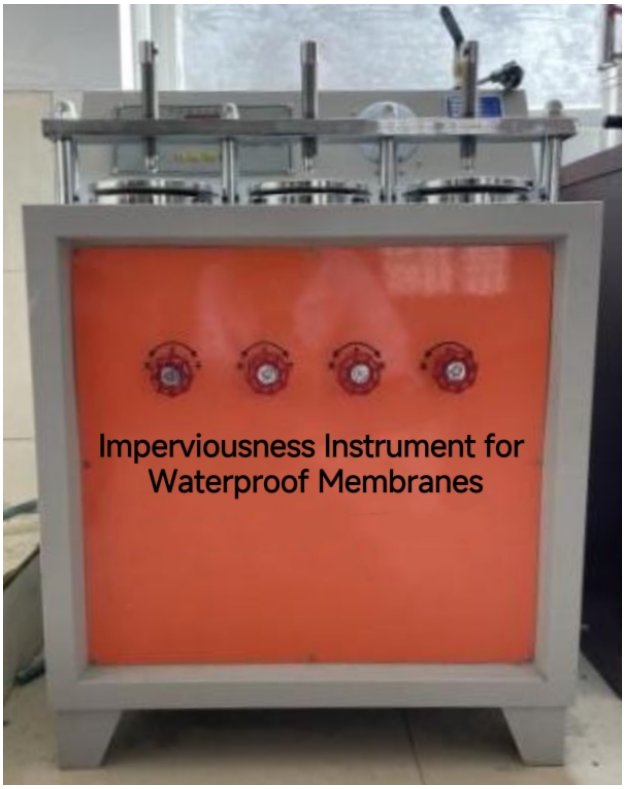

Fig. 4. Imperviousness Instrument for Waterproof Membranes

Fig. 5. Installation-Effect Diagram of the Film

4. Result Analysis and Discussion

4.1 Analysis of Orthogonal Test Results

Results of the three-factor four-level orthogonal test table (Table 1) are presented in Table 2.

Table 2 Orthogonal Test Results

Example	Tensile Strength (MPa)	Elongation at Break (%)	Bonding Strength (MPa)
1	1.33	69	1.4
2	1.42	90	1.1
3	1.58	130	0.7
4	1.62	150	0.5
5	1.65	54	1.20
6	1.69	62	1.23
7	1.72	83	1.35
8	1.84	117	1.36

9	2.2	67	1.32
10	2.34	73	1.45
11	2.6	84	1.62
12	2.43	93	1.53
13	2.76	43	1.4
14	2.84	51	1.8
15	2.97	59	1.9
16	3.1	70	2.2

Through the range analysis of the orthogonal test results in Tables 3 and 4, the primary and secondary order of factors affecting tensile strength and elongation at break was as follows: styrene–acrylic emulsion > pure-acrylic emulsion > cement.

Tables 3 and 4 indicate that the styrene–acrylic emulsion exerts the greatest impact on the mechanical properties of the waterproofing coating. This was because the styrene–acrylic emulsion with styrene segments introduced enhanced the stain resistance and physical and mechanical properties of the acrylic emulsion after film formation, thereby increasing the tensile strength of the dried coating. As the mass ratio of the styrene–acrylic emulsion increased, the tensile strength of the waterproofing coating also increased, resulting in decreased elongation at break.

Table. 3. Range Analysis of Tensile Strength in Orthogonal Test

1 Sum of Horizontal Indicators	5.95	7.94	8.72
2 Sum of Horizontal Indicators	6.9	8.29	8.47
3 Sum of Horizontal Indicators	9.57	8.87	8.46
4 Sum of Horizontal Indicators	11.67	8.99	8.44
1 Horizontal Average Value	1.4875	1.985	2.18
2 Horizontal Average Value	1.725	2.0725	2.1175
3 Horizontal Average Value	2.3925	2.2175	2.115
4 Horizontal Average Value	2.9175	2.2475	2.11
Range	1.43	0.2625	0.07
Primary and Secondary Order	Styrene–Acrylic Emulsion>Pure-acrylic emulsion>Cement		

Table 4. Range Analysis of Elongation at Break in Orthogonal Test

1 Sum of Horizontal Indicators	439	233	285
2 Sum of Horizontal Indicators	316	276	296
3 Sum of Horizontal Indicators	317	356	365
4 Sum of Horizontal Indicators	223	430	349
1 Horizontal Average Value	109.75	58.25	71.25
2 Horizontal Average Value	79	69	74
3 Horizontal Average Value	79.25	89	91.25
4 Horizontal Average Value	55.75	107.5	87.25
Range	54	49.25	20
Primary and Secondary Order	Styrene–Acrylic Emulsion>Pure-acrylic emulsion>Cement		

Table 5. Range Analysis of Bonding Strength in Orthogonal Test

1 Sum of Horizontal Indicators	3.7	5.32	6.45
2 Sum of Horizontal Indicators	5.14	5.58	5.73
3 Sum of Horizontal Indicators	5.92	5.57	5.18
4 Sum of Horizontal Indicators	7.3	5.59	4.7
1 Horizontal Average Value	0.925	1.33	1.6125
2 Horizontal Average Value	1.285	1.395	1.4325
3 Horizontal Average Value	1.48	1.3925	1.295
4 Horizontal Average Value	1.825	1.3975	1.175
Range	0.9	0.0675	0.4375
Primary and Secondary Order	Styrene–Acrylic Emulsion>Cement>Pure-acrylic emulsion		

Tables 3 and 4 evidently show that the styrene–acrylic emulsion exerts the most significant impact on the mechanical properties of the waterproofing coating. This was because, the styrene–acrylic emulsion with styrene segments introduced enhanced the stain resistance and physical and mechanical properties of the acrylic emulsion after film formation. With increased mass ratio of the styrene–acrylic emulsion, the tensile strength of the waterproofing coating increased, whereas the elongation at break decreased. Conversely, the pure-acrylic emulsion exerted an impact on the mechanical properties of the waterproofing coating second only to the styrene–acrylic emulsion. The pure-acrylic emulsion boasted good flexibility, which improved the elongation at break and excellent weather resistance and safety. As the content of the pure-acrylic emulsion increased, the elongation at break and bonding strength increased constantly, whereas the tensile strength decreased.

Table 5 shows that cement significantly affected the bonding strength of the waterproofing coating second only to styrene acrylic. The reason was that during the bonding-strength test, the material of the base specimen was cement mortar. The cement in the coating had strong hydration activity, resulting in high bonding strength, which allowed for excellent bonding with the base specimen, thereby enhancing the bonding strength of the waterproofing coating.

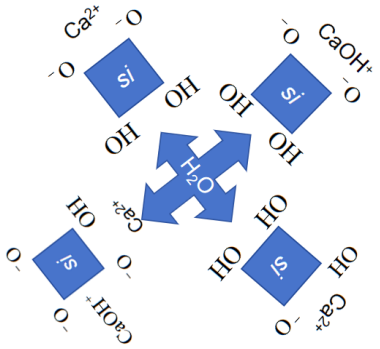

Fig. 6. Schematic of Cement Hydration Ion Binding

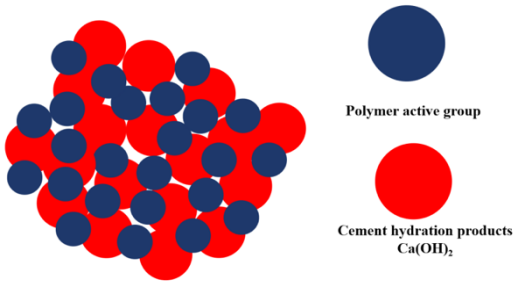

Fig. 7. Schematic of Macromolecular Network Structure

Fig. 6 and 7 show that the polymer-active groups underwent hydration reaction with cement, altering the interface effect with concrete and enhancing material properties through the interface. The polymer emulsion can form a macromolecular network structure with cement hydration, bonded by ionic bonds. With increased hydration time, the hydration reaction became more complete, thereby further improving the mechanical properties.

Polymers with functional groups such as -COOH can interact with the cement hydration product Ca^{2+}, significantly enhancing the strength and water resistance of the material. Polymer and cement played active (reactive)

roles. The presence of chemical bonds between the polymer and cement interface tremendously strengthened the interface bonding, increasing the load-bearing capacity of the interface and thus improving the interface toughness and fracture energy. The outcomes were excellent physical and mechanical properties.

Styrene–acrylic emulsion and pure-acrylic emulsion did not undergo chemical reactions, demonstrating good compatibility and forming a complementary effect. In the performance testing of the film, waterproofing coatings prepared solely from pure acrylic exhibited insufficient rigidity, whereas those prepared solely from styrene–acrylic had poor elongation at break. Thus, by compounding styrene acrylic and pure acrylic, the combined rigidity of styrene acrylic and flexibility of pure acrylic enabled the preparation of high-quality waterproofing coatings with excellent elongation at break, sufficient bonding strength, and tensile strength.

In the first phase, cement was uniformly distributed in the styrene–acrylic emulsion, forming styrene–acrylic cement slurry. As hydration proceeded, a segment of the styrene-acrylic emulsion was deposited within the hydration products. In the second phase, hydration products gradually formed, and the styrene–acrylic emulsion was restricted within the capillaries, with the moisture in the capillaries reduced due to cement hydration. The styrene–acrylic emulsion accumulated, forming a densely packed lamellar structure. In the third phase, the styrene–acrylic emulsion coalesced into a film, together with the hydration products, a pervasive network structure formed. Due to a certain rigidity of the styrene–acrylic emulsion, the tensile strength of the film was enhanced. Similarly, in the second phase, pure-acrylic emulsion accumulated, forming a densely packed lamellar structure. In the third phase, pure-acrylic emulsion coalesced into a film, together with the hydration products, a pervasive network structure formed. The excellent bonding strength of the pure-acrylic emulsion ensured the bonding strength of the film and elongation at break.

The orthogonal test results showed that groups 11 and 12 had the optimal comprehensive properties of waterproofing-coating materials in terms of tensile strength, elongation at break, and bonding strength.

4.2 Impact of Different Cement Grades on the Property of Waterproofing-Coating Material

Based on the experimental methods in 3.3, a comparative test was conducted on group 11 in the orthogonal test. This group exhibited superior physical and mechanical properties and imperviousness. This allowed for the selection of the optimal cement grade and an investigation of the impact on its tensile strength, elongation at break, bonding strength, and imperviousness.

Using different grades of cement according to the formula design of groups 11 and 12 from the orthogonal test table, we found through extensive tests that the film surface exhibited cracking issues after drying (Fig.s 8 and 9). After analysis and summarization, the causes of cracking were elucidated as follows. (1) Too high humidity in the laboratory caused the water molecules in the air to gradually enter the surface of the film being cured, delaying the speed and time of film formation and drying and causing the continuation of hydration reactions in a few parts that have not yet dried, leading to non-uniform cracking of the entire film. (2) The film was applied too thickly at the first time, resulting in a large temperature difference between the inside and outside of the film. The outside was unable to promptly release the heat generated internally, thereby causing film cracking. (3) In the stirred tank, the amount of dispersant was insufficient, leading to uneven dispersion of inorganic fillers and cement in the coating during application, causing inconsistencies in the hydration reaction during film formation and eventual cracking. (4) Inorganic fillers such as cement clumped together when exposed to moisture. Even after rapid stirring, a significant number of visible small particles remained in the stirred tank. During film formation, the coating encapsulated a large amount of inorganic fillers. Thus, when drying, the particles needed to absorb a considerable amount of water from the emulsion, leading to cracking around the particles. (5) The release agent for the film (chlorinated paraffin) was too thick. When the coating was evenly applied over it, the excessively thick chlorinated paraffin penetrated the film. It was an oil-based material, so it did not crosslink with the coating and formed small areas of contamination. When drying, the boundary between the two was the most prone to cracking. (6) Considering that the setting time of the cement was too fast and the hydration reaction was intense, when the coating was drying, overall uneven cracking occurred. The reason was the excessive temperature difference between the inside and outside, as well as the excessive surface tension.

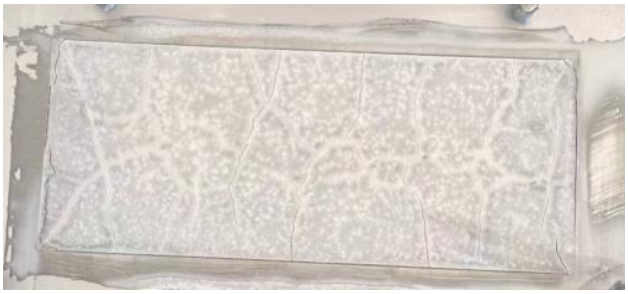

Fig. 8. Overall Cracking of the Film

Fig. 9. Cracking of a Small Part of the Film

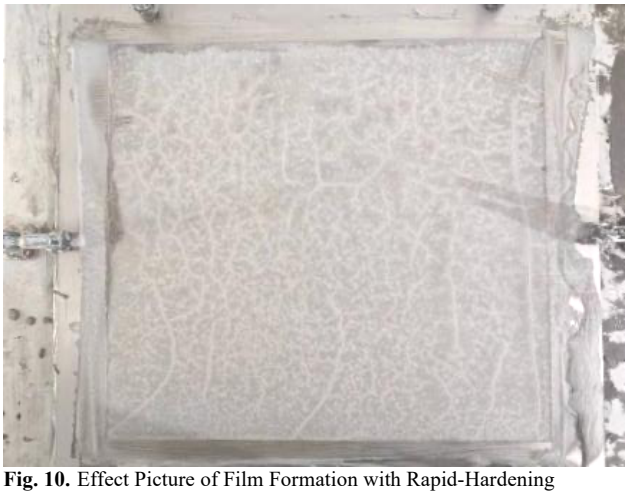

Fig. 10. Effect Picture of Film Formation with Rapid-Hardening Sulfate–aluminate cement

Fig. 11. Effect Picture of Film Formation with Rapid-Hardening Sulfate–aluminate cement

Under standard test conditions and with the test process fully compliant, the issues of (1), (4), and (5) mentioned above were excluded. Comparative tests were conducted using different grades of ordinary silicate cement and the rapid-hardening sulfate–aluminate cement. As shown in Fig.s 10 and 11, when using the rapid-hardening sulfate–aluminate cement, the hydration reaction was too rapid. A large amount of heat was released, leading to a significant temperature difference between the inside and outside of the film. This caused uneven surface heat dissipation and excessive surface tension, preventing the emulsion from acting as a crosslinking agent. Consequently, numerous cracks appeared on the film surface, rendering it unsuitable for further testing. Considering this comprehensively, the study and analysis of the rapid-hardening sulfate–aluminate cement were abandoned. Considering the aforementioned issues, this study began on the C32.5, C42.5, and C52.5 cements, with tests conducted according to the formula design of groups 11 and 12 from the orthogonal test table, investigating the tensile strength, elongation at break, and impermeability.

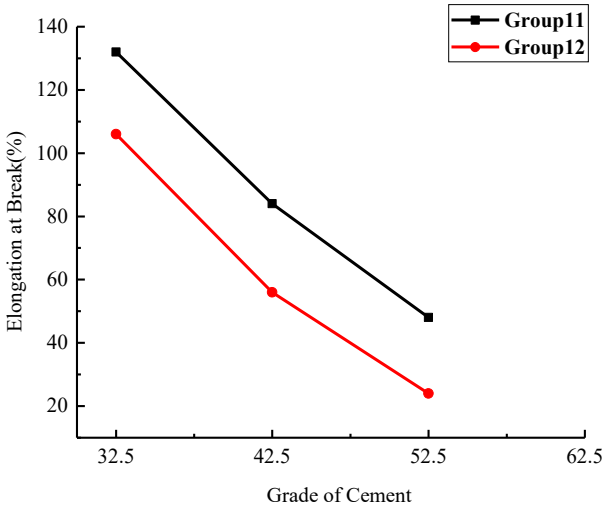

Fig. 12. Test Results of Cement Grade Against Tensile Strength

Through experiments, the regular patterns of different cement grades on tensile strength and elongation at break were obtained. As shown in Fig. 12, the tensile strength generally increased with continuously increased cement grade. Analysis results indicated that a higher cement grade led to a higher tensile strength of the waterproof film when forming cement slurry after hydration and curing. Fig. 13 shows that the elongation at break generally decreased. The emulsion can maintain a good elongation at break, but the strength increased with increased cement grade, and the emulsion cannot fully crosslink the higher grade cement. Some cement underwent complete hydration reaction. Due to their excessive strength, during the elongation at break test, sudden fractures often occurred at high-strength areas, leading to a decrease in the elongation at break of the film. Fig. 14 reveals that the bonding strength also increased with increased cement grade. A higher cement grade led to a stronger crosslinking hydration reaction with the old surface of the bonding surface, making the bonding surface more compact. Thus, during the bonding-strength test, a higher cement grade led to a higher bonding strength of the specimen. Based on a comprehensive analysis, considering that the elongation at break of group 12 was too low, group 11 with C42.5 ordinary silicate cement was selected as the optimal mix ratio.

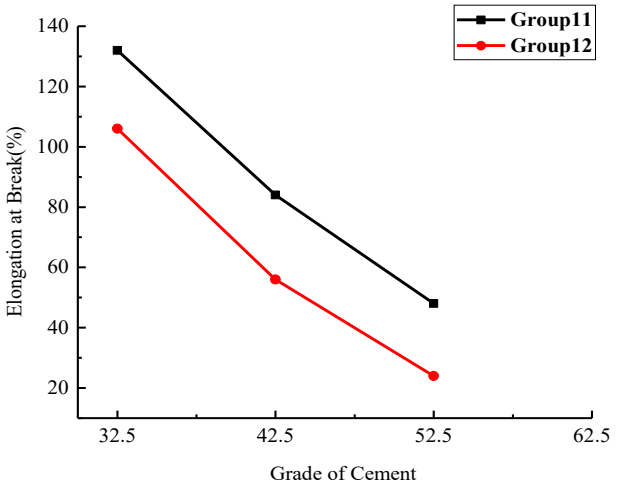

Fig. 13. Test Results of Cement Grade Against Elongation at Break

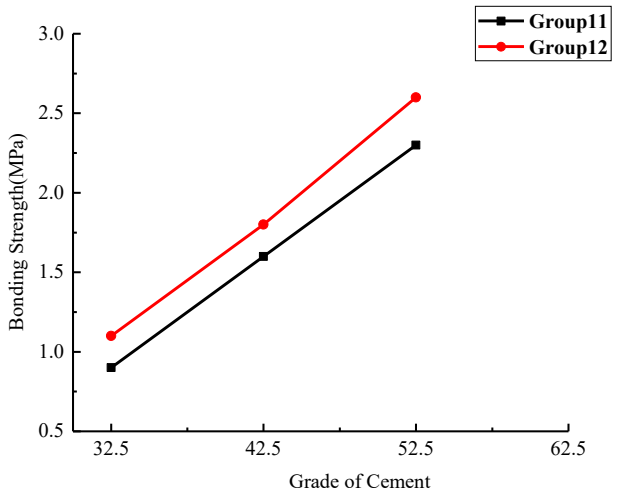

Fig. 14. Test Results of Cement Grade Against Bonding Strength

Table 6. Test for Imperviousness

Cement Grade	32.5	42.5	52.5	Rapid-Hardening Sulfate–Aluminate
Group 11	Qualified	Qualified	Unqualified	Unqualified

Table 6 shows that according to the test formula design of group 11, all specimens except those using C52.5 ordinary silicate cement (Fig. 15) and the rapid-hardening sulfate–aluminate cement passed the impermeability test. Fig. 16 shows the qualified imperviousness conditions on the back side of the specimens in group 11. The perviousness was characterized by the test sealing ring spreading outwards and pervious to water, with impermeability pressure rising against the water-facing side, causing the originally smooth specimen to bulge along the sealing ring. Consequently, the film surface became convex, making the sealing ring and small circle the most vulnerable locations for damage. Fig. 15 shows that the surface of the impermeability failure was generally around the sealing ring and small circle. This was because the water pressure cannot maintain its rigidity, leading to a certain deformation. C52.5 cement had a high rigidity, making it unable to resist the deformation caused by water pressure, resulting in the specimen being gradually broken from the sealing ring and small circle as the pressure kept rising, thereby penetrating the back side and leading to test failure.

Fig. 15. Impermeability Test of C52.5 Cement

Fig. 16. Back Side Bulging of the Specimen

4.3 Impact of Waterborne Non-Silicone Defoamer on the Property of Waterproofing-coating materials

Based on the experimental methods in 3.1, we concluded that the bubbles in the film significantly decreased with increased amount of the waterborne non-silicone defoamer used. Specimens with different amounts of admixture of waterborne non-silicone defoamer were cut into impervious specimens and subjected to impermeability tests (Table 7). With increased dosage of the waterborne non-silicone defoamer, the bubbles in the coating rapidly disappeared. When the defoamer accounted for 0.3% of the liquid component, the section of the film had no obvious bubbles, and the internal microspaces were reduced. According to the principle, the waterborne non-silicone defoamer can quickly diffuse in the coating, reducing its surface tension and causing the bubbles to disappear rapidly. Thus, as shown in Table 7, when no defoamer was added, the coating had a porous internal structure, which created water-permeation channels under water pressure, leading to water perviousness of the specimen.

Table 7. Test of Dosage of Waterborne Non-Silicone Defoamer Against Imperviousness

Mass Ratio of Dosage of Defoamer (%)	**0**	**0.15**	**0.3**	**0.45**	**0.6**
Imperviousness	Unqualified	Unqualified	Unqualified	Unqualified	Unqualified

As depicted in Fig. 17, the tensile strength gradually improved with increased defoamer content, reaching a stable state at a dosage of 0.3% defoamer. The reason was that the 0.3% defoamer eliminated overall bubbles in the coating, reducing microscopic voids, and thereby increasing the film compactness, resulting in improved tensile strength (Fig. 17). Fig. 18 shows that the defoamer exerted a significant impact on the elongation at break of the film, increasing to 104% as the dosage of the defoamer increased. This was due to the increased compactness of the waterproof film with increased amount of defoamer used. In the process of uniform tensile fracture, the coated specimen transitioned from a dense state into a loose one before fracturing, leading to increased elongation at break of the specimen as the internal defects of the film decreased. Fig. 19 reveals that the bonding strength also gradually improved with increased defoamer dosage; when it was too low, the internal compactness of the film was insufficient, often resulting in failure from the middle of the film during the bonding-strength test (Fig. 20). Consequently, the test results were affected. Furthermore, the overall compactness inside the film increased with continuously increased defoamer content, reducing the number of small internal voids. The outcome was a substantial improvement in the film property.

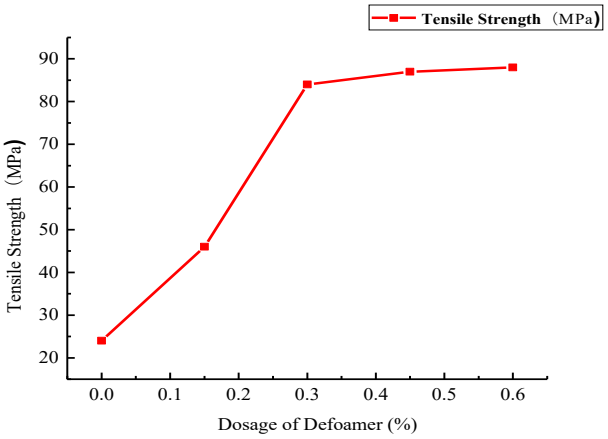

Fig. 17. Impact of Defoamer Dosage on Tensile Strength

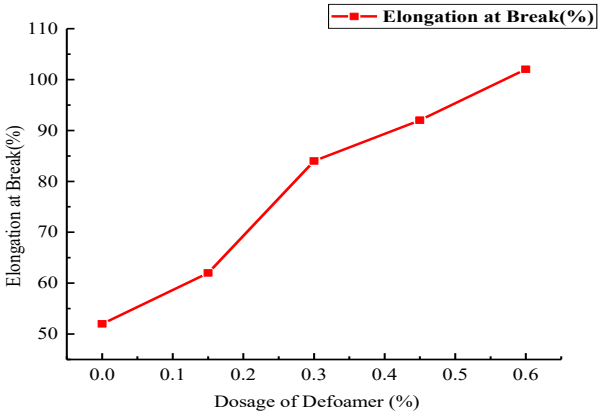

Fig. 18. Impact of Defoamer Dosage on Elongation at Break

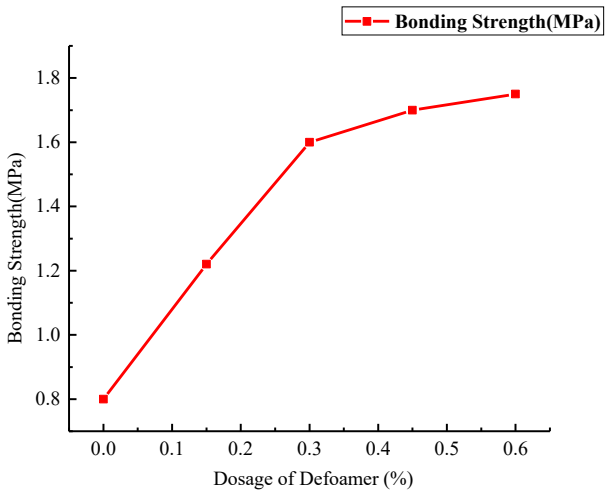

Fig. 19. Impact of Defoamer Dosage on Bonding Strength

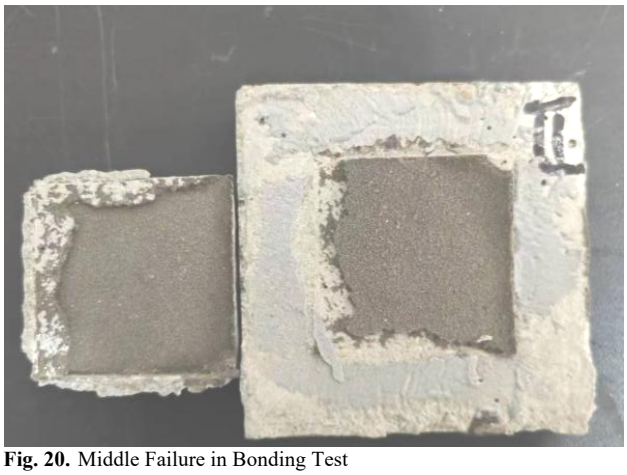

Fig. 20. Middle Failure in Bonding Test

The two-component waterborne polymer-cement waterproof material studied in this paper had a tensile strength of 2.6 MPa, an elongation at break of 84%, and bonding strength of 1.6 MPa when the defoamer dosage was 0.3%. These features provided a high-bonding strength acrylic-polymer waterproof material with a designed mix ratio capable of withstanding a certain degree of settlement and cracking for the required water resistance and impermeability of underground engineering.

5. Conclusions

To enhance the property of acrylic-polymer waterproofing materials and elucidate the advantages and challenges of waterproofing materials for underground engineering, this study established an orthogonal experimental model by compounding pure-acrylic emulsion and styrene–acrylic emulsion. We analyzed the optimal mix ratio of the two-component acrylic-polymer waterproofing material, the impact of cement grade on the property of underground waterproofing coatings, and the impermeability characteristics of the waterproofing coating for underground engineering. The following conclusions can be drawn.

(1) When pure-acrylic emulsion and styrene–acrylic emulsion accounted for 65% and 27%, respectively, the prepared waterproofing coating underwent an imperviousness test without water permeation under 0.3MPa water pressure. Moreover, the physical and mechanical properties were stable, and the production cost was significantly lowered.

(2) The percentages of dispersant, defoamer, and thickener in the liquid component were fixed at 0.2%, 0.3%, and 0.3%, respectively. The solid components included C42.5 ordinary silicate cement, 80–120 mesh quartz sand, 200 mesh quartz powder, 400 mesh heavy calcium carbonate, 800 mesh heavy calcium carbonate, and 1250 mesh talc powder, each of which constituted 35%, 30%, 15%, 12%, 6%, and 2% of the solid component, respectively. In this phase, the mass ratio of the liquid component to the solid component was 1:1.5. The improvement in the mechanical properties of the coating was positively correlated with the cement grade, with the best comprehensive properties observed when using C42.5 cement. The tensile strength was 2.6MPa, the elongation at break was 84%, and the bonding strength was 1.6MPa.

(3) The percentages of dispersant, defoamer, and thickener in the liquid component were fixed at 0.2%, 0.3%, and 0.3%, respectively. The solid components included C42.5 ordinary silicate cement, 80–120 mesh quartz sand, 200 mesh quartz powder, 400 mesh heavy calcium carbonate, 800 mesh heavy calcium carbonate, and 1250 mesh talc powder, each of which constituted 35%, 30%, 15%, 12%, 6%, and 2% of the solid component, respectively. The waterborne non-silicone defoamer effectively reduced bubbles in the acrylic-polymer waterproofing coating, enhancing its compactness and reducing microscopic voids within the coating. With increased amount of the waterborne non-silicone defoamer used, the elongation at break and the bonding strength of the waterproofing coating exhibited a positive correlation with the defoamer dosage. The elongation at break reached the maximum of 104%, and the bonding strength reached the maximum of 1.8MPa. Furthermore, when the defoamer dosage was over 0.3%, the imperviousness effect of the waterproof coating film was excellent.

Based on an analysis of the advantages and disadvantages of waterproofing materials for underground engineering, in combination with theoretical and experimental data, we proposed a high-bonding acrylic polymer waterproof material by compounding pure-acrylic emulsion and styrene–acrylic emulsion. Our results provided a reference for the promotion and application of acrylic-polymer waterproof materials for underground engineering and offered a mix-ratio design of waterproofing coatings that can resist a certain degree of settlement and cracking and have high bonding strength.

Acknowledgements
This work was supported by the National Natural Science Foundation of China (Grant No.52279134); Sponsored by Natural Science Foundation of Henan (Grant No. 232300420323); China Ministry of Education industry-university cooperative education project (Grant No. 231007228085539).

References

[1] F. W. Zhu *et al*, "Advances in waterproofing technology for urban underground engineering," *Constr. Technol.*, vol. 48, no. 21, pp. 43-46+69, Nov. 2019.

[2] D. Yan, S. B. Chen, X. D. Xiao, F. X. Zhang, and I. C. Chen, "Characteristics of a Two-component Waterborne Acrylic Emulsion Waterproof Coating based on Underground Engineering," *J. Eng. Sci. Technol. Rev.*, vol. 15, no. 03, pp. 99-108, Jun. 2022.

[3] X. Liu, X. W. Xiao, H. T. Xu, and H. L. Lu, "Analysis of the development status and countermeasures of waterproof engineering in China," *Constr. Technol.*, vol. 50, no 03, pp. 5-8, Feb. 2021.

[4] D. L. Liu, Y. Y. Huang, J. L. Zheng, J. B. Yuan, and Y. Q. Liu, "Study of mechanism of flame-retardant SBS-modified asphalt," *Int. J. Pavement Res. Technol.*, vol. 02, no. 04, pp. 162-165, Jul. 2009.

[5] M. Guo *et al*, "Study on water permeability, shear and pull-off performance of waterproof bonding layer for highway bridge," *Constr. Build. Mater.*, vol. 11 no. 04, pp. 396-400, Jul. 2018.

[6] Y. J. Jiang, L. Lei, H. S. Wang, R. Wang, and Q. Tian, " Influence of Acrylic Emulsion on Polymer-Cement Waterproof Coating," *A. M. R.* vol. 1129, pp. 263-269, Nov. 2015.

[7] F. Y. Yan and C. Y. Zhao, "Mechanism and application progress of polymer cement waterproofing coatings," *Plat. Finish.*, vol. 34 no. 09, pp. 25-28+33, Sep. 2012.

[8] H. Wu, Y. Q. Deng, W. Yang, T. Wu, and S. Jia, "Preparation of waterborne micro-nano graphene polymer cement waterproofing coatings," *Ind. Miner. Process.,* vol. 51, no. 03, pp. 41-44+59, May. 2021.

[9] G. Cheng, Y. Zhou, and G. W. Zhang, "Preparation and property study of formaldehyde-free acrylate polymer cement waterproofing coatings," *Paint. Coat. Ind.*, vol. 46, no. 03, pp. 52-56+63, Mar. 2016.

[10] L. Czarnecki and J. J. Sokołowska, "Optimization of Polymer-Cement Coating Composition Using Material Model," *Key Eng. Mater.*, vol. 466, pp. 191-199, Jan. 2011.

[11] R. Wang, D. X. Ma, P. M. Wang, and G. Y. Wang, "Study on waterproof mechanism of polymer-modified cement mortar," *Mag. Concr. Res.*, vol. 67, no. 18, pp. 972-979, Sep. 2015.

[12] Y. R. Kim, H. J. Ko, J. S. Park, D. B. Kim, and S. W. Lee, "A Study on the Crack Response and Waterproof Properties of High-Functional Water-Based Acrylic Paints for Exterior Walls," *Koera Build. Constr.*, vol. 21, no. 06, pp. 593-604, Dec. 2021.

[13] J. Y. Lee, J. K. Choi, and S. S. Kim, "Examination of Tensile and Adhesion Property According to Components and Application Environment of Cement-mixed Polymer-based Waterproofing," *J. Korea Inst. Struct. Maint. Insp.*, vol. 25, no. 06, pp. 41-49, Dec. 2021.

[14] Y. Meng *et al,* "A fluoride-free hydrophobic composite coating with mechanical robustness and anti-UV aging," *J. Mater. Sci.*, vol. 58, pp. 3534-3550, Feb. 2023.

[15] B. J. Liu and D. Liang, "Effect of mass ratio of asphalt to cement on the properties of cement modified asphalt emulsion mortar," *Constr. Build. Mater.*, vol. 134, pp. 39-43, Mar. 2017.

[16] M. M. Al-Zahrani, S. U. Al-Dulaijan, M. Ibrahim, H. Saricimen, and F. M. Sharif, "Effect of waterproofing coatings on steel reinforcement corrosion and physical properties of concrete," *Cem. Concr. Compos.*, vol. 24, no. 01, pp. 127-137, Feb. 2002.

[17] A. Marques, J. G. Lopes, and J. R. Correia, "Durability of the adhesion between bituminous coatings and self-protection mineral granules of waterproofing membranes," *Constr. Build. Mater.*, vol. 25, no. 01, pp. 138-144, Jan. 2011.

[18] F. F. Yu, X. Xu, N. B. Lin, and X. Y. Liu, "Structural engineering of waterborne polyurethane for high performance waterproofing coatings," *RSC Adv*., vol. 05, no. 89, pp. 72544-72552, Aug. 2015.

[19] M. Jassal, A. Khungar, P. Bajaj, and T. J. M. Sinha, "Waterproof breathable polymeric coatings based on polyurethanes," *J. Ind. Text.*, vol. 33, no. 04, pp. 213-281, Apr. 2004.